RESEARCH PAPERS

Unmanned Aerial Vehicle (UAV)-based remote sensing to monitor grapevine leaf stripe disease within a vineyard affected by esca complex

Salvatore F. DI GENNARO[1], Enrico BATTISTON[2], Stefano DI MARCO[3], Osvaldo FACINI[3], Alessandro MATESE[1], Marco NOCENTINI[2], Alberto PALLIOTTI[4] and Laura MUGNAI[2]

[1] Istituto di Biometeorologia (IBIMET), CNR, Via G. Caproni 8, 50145 Firenze, Italy
[2] Dipartimento di Scienze delle Produzioni Agroalimentari e dell'Ambiente (DiSPAA) - Sez. Patologia vegetale ed Entomologia, Università degli Studi di Firenze, Piazzale delle Cascine 28, 50144 Firenze, Italy
[3] Istituto di Biometeorologia (IBIMET), CNR, Via Gobetti 101, 40129 Bologna, Italy
[4] Dipartimento di Scienze Agrarie e Ambientali, Università degli Studi di Perugia, Borgo XX Giugno 74, 06128 Perugia, Italy

Summary. Foliar symptoms of grapevine leaf stripe disease (GLSD, a disease within the esca complex) are linked to drastic alteration of photosynthetic function and activation of defense responses in affected grapevines several days before the appearance of the first visible symptoms on leaves. The present study suggests a methodology to investigate the relationships between high-resolution multispectral images (0.05 m/pixel) acquired using an Unmanned Aerial Vehicle (UAV), and GLSD foliar symptoms monitored by ground surveys. This approach showed high correlation between Normalized Differential Vegetation Index (NDVI) acquired by the UAV and GLSD symptoms, and discrimination between symptomatic from asymptomatic plants. High-resolution multispectral images were acquired during June and July of 2012 and 2013, in an experimental vineyard heavily affected by GLSD, located in Tuscany (Italy), where vines had been surveyed and mapped since 2003. Each vine was located with a global positioning system, and classified for appearance of foliar symptoms and disease severity at weekly intervals from the beginning of each season. Remote sensing and ground observation data were analyzed to promptly identify the early stages of disease, even before visual detection. This work suggests an innovative methodology for quantitative and qualitative analysis of spatial distribution of symptomatic plants. The system may also be used for exploring the physiological bases of GLSD, and predicting the onset of this disease.

Key words: precision viticulture, disease detection, asymptomatic plant, trunk disease.

Introduction

Fungal trunk diseases (mainly Eutypa dieback, Botryosphaeria dieback, esca complex) are responsible for significant economic losses to the wine industry worldwide, and are the most difficult grapevine diseases to control (Di Marco *et al.,* 2011a). Among these diseases esca complex is the most widespread in Europe (Surico *et al.*, 2008; Bertsch *et al.*, 2013; Gubler *et al.*, 2015), including wood decay (in Europe mainly caused by *Fomitiporia mediterranea*) and grapevine leaf stripe disease (GLSD) mainly associated with wood vascular infections by *Phaeomoniella chlamydospora* and *Phaeoacremonium minimum* ("*P. aleophilum"*, *sensu* Gramaje *et al.*, 2015*)*, but also with a not yet well characterized vascular disfunction. In older vines, wood decay and GLSD frequently occur together on the same plant (Mugnai *et al.*, 1999; Surico *et al.*, 2008; Andolfi *et al.*, 2011). Symptoms of GLSD include foliar interveinal necrosis, giving affected leaves the typical tiger-stripe appearance (Figure 1). Affected vines produce poor quality grapes

Corresponding author: S.F. Di Gennaro
E-mail: f.digennaro@ibimet.cnr.it

Figure 1. Typical foliar symptoms of grapevine leaf stripe disease (GLSD) show interveinal chlorosis and/or necrosis, typically surrounded by a reddish, purple or yellow margin. While there is variability in the appearance of symptoms in different cultivars, the so called "tiger stripe" pattern is fairly typical.

(Calzarano *et al.*, 2004b; Lorrain *et al.*, 2012), have reduced production and a high incidence of yearly death, representing an increasing threat for grape growers around the world, but especially in Europe (Bertsch *et al.*, 2013; Gubler *et al.*, 2015).

The most typical characteristics of GLSD are the absence of correlation between the severity of wood deterioration and the appearance and severity of leaf symptoms (Calzarano *et al.*, 2007; Fontaine *et al.*, 2016), and the intermittent expression of leaf symptoms. These may not appear in every growing season on each affected same vine, even if it is infected and has shown symptoms in previous years. This discontinuity of leaf symptoms on individual vines makes it extremely difficult to determine the true incidence of the disease in a vineyard at any given time because many infected vines may not show symptoms every year (Surico *et al.*, 2000; Marchi *et al.*, 2006). As a consequence, annual monitoring of leaf symptoms becomes fundamental for evaluating disease expression over progressive years, and to acquire cumulative indices of the real incidence of the disease. A plant affected by GLSD or, in general terms, by esca disease, can give normal production if it remains symptomless in that year. Thus, it is only the manifestation of symptoms that is directly related to a loss of quality of the final product in each year (Calzarano *et al.*, 2004b), besides leading to a progressive weakening and finally to death of the vine.

There is considerable debate about the factors leading to development of foliar symptoms (Fontaine *et al.*, 2016). These include the possible involvement of phytotoxic substances (Andolfi *et al.*, 2011) produced by the pathogens, a relevant role of environmental factors, specifically rain (Marchi *et al.*, 2006), and general vascular dysfunction triggered by inappropriate cultural practices (Lecomte *et al.*, 2012). Whatever the causes (most probably a combination of factors) many authors have demonstrated drastic alteration of photosynthetic functions as well as stimulation of defense responses in affected grapevines several days before the appearance of the first foliar symptoms (Bertamini *et al.*, 2002; Christen *et al.*, 2007; Letousey *et al.*, 2010; Mattii *et al.*, 2010; Magnin-Robert *et a1.*, 2011; Calamai *et al.*, 2014). Early detection of a disease is important in studies of symptom development, and for evaluation of the efficacy of the few control strategies available (Di Marco *et al.*, 2011b; Calzarano *et al.*, 2014; Smart, 2015). Early

detection can also support understanding of the factors that incite symptom development, leading to prevention of yield and quality losses. Furthermore, despite the general lack of effective control methods, early detection of symptomatic vines can enhance effectiveness of local trunk treatment or management (Lafon, 1921; Calzarano *et al*., 2004a; Darrieutort and Lecomte, 2007; Smart, 2015).

The strong relationship between foliar symptoms and alteration of photosynthetic activity has been the key to suggest new methodology to investigate the onset of symptoms, based on optical techniques aimed to monitor parameters linked to leaves, and therefore host physiological state. Recent developments in optical technology have provided rapid and non-destructive methods for disease detection based on reflectance data and spectral vegetation indices (Johnson *et al*., 1996; Zhang *et al*., 2002; Bravo *et al*., 2003; Steddom *et al*., 2003; Steddom *et al*., 2005; Graeff *et al*., 2006; Delalieux *et al*., 2007; Huang *et al*., 2007; Larsolle and Muhammed, 2007; Delalieux *et al*., 2009; Naidu *et al*., 2009; Wang *et al*., 2009; Sankarana *et al*., 2010; Reynolds *et al*., 2012; Bellow *et al*., 2013; Mirik *et al*., 2013; Berdugo *et al*., 2014; Elarab *et al*., 2015; Martinelli *et al*., 2015). In particular, plant spectral properties at visible and near-infrared wavelengths can assist development of specific signatures for specific stresses in different species (Hatfield and Pinter, 1993; Peñuelas and Filella, 1998; West *et al*., 2003). The green vegetation spectral reflectance in the red band is most sensitive to leaf chlorophyll content, while the near infrared band is most related to biomass (Thomas and Oerther, 1972; Toler *et al*., 1981; Blazquez and Edwards, 1983; Kurschner *et al*., 1984; Blakeman, 1990). In that respect, the Normalized Difference Vegetation Index (NDVI) is a good parameter to evaluate leaf chlorophyll content, which is directly correlated with the health status of plants. NDVI is calculated from the following equation:

$$NDVI = (\varrho NIR - \varrho R) / (\varrho NIR + \varrho R)$$

where ϱNIR and ϱR are, respectively, the reflectance in near infra-red and red bands (Rouse *et al*., 1973). An example is the work of Bauer *et al*. (2011), which described a laboratory method to provide early and reliable detection of sugar beet leaf diseases based on high resolution multispectral images realized with Tetracam ADC-Lite. Since the end of the 1960s remote sensing has been used in plant disease detection with increasing frequency. Remote sensing techniques are replacing traditional methods in field or laboratory analysis when repetitive large-scale measurements are required, representing the only feasible approach for obtaining these data (Steven and Clark, 1990; Fitzgerald *et al*., 2004). Even from early reports, many authors have suggested that remote sensing could be used for provisional plant disease detection some days before visual symptoms became apparent (Manzer and Cooper, 1967; Burns *et al*., 1969). Those observations could be applicable also for GLSD or esca complex of grapevine (Christen *et al*., 2007; Mattii *et al*., 2010; Magning-Robert *et al*., 2011).

The principle on which remote sensing techniques is based in plant disease detection is to investigate physiological disturbances by recording changes in foliar reflectance in the near infrared portion of the spectrum, which is not perceptible by eye. Thus, remote sensing provides a quick and low cost tool to analyze biotic and abiotic stress from differences in the spectral characteristics of the crop canopy. The performance of aircraft remote sensing in precision viticulture is well explored (Johnson *et al*., 1996; Johnson *et al*., 2003b; Hall *et al*., 2003). The approach is currently increasing in flexibility and spatial resolution of up to 0.4 m per pixel, as compared with satellite platforms, which at most reach resolution of 1.2 m per pixel in multispectral bands (Worldview-3). However, disease detection requires greater spatial resolution (Calderón *et al*., 2013) in order to discriminate row from inter-row, and even each vine within a row. Technological automation developments have provided a new solution for remote monitoring, the Unmanned Aerial Vehicles (UAVs). These fixed-wing or rotary platforms can be remotely controlled by a pilot or fly autonomously on user-planned routes by means a complex flight control sensors. The key strength of UAV application in remote sensing is the high spatial ground resolution (centimeters), and a reduced planning time, which allows for highly flexible and timely monitoring (Johnson *et al*., 2003a; Baluja *et al*., 2012; Colomina and Molina, 2014; Mathews 2014; Matese *et al*., 2015; Mathews, 2015; Zaman-Allah *et al*., 2015).

Since 2011, the Precision Viticulture group of the Institute of Biometeorology of the National Research Council, in collaboration with the Section of Plant pathology and Entomology (DISPAA, University of Florence), has carried out a series of experiments focused on GLSD in a vineyard in Chianti Classico

Domain (Tuscany, Italy). The purpose was to study the relationships between NDVI, derived from high resolution images acquired by UAV platforms, and symptomatic plants monitored by ground based observations. Despite the general lack of clear and consistent explanations of the factors that incite foliar symptoms, one aspect that is widely accepted is the role of rain in late spring-early summer in increasing the appearance of GLSD symptoms (Marchi *et al.*, 2006; Guérin-Dubrana *et al.*, 2012; Andreini *et al.*, 2015). The years 2012 and 2013 differed markedly for summer rain parameters, so it is relevant to compare the data obtained by the UAV surveys in those two years. A second objective was to develop an innovative methodology aimed primarily at quantitative and qualitative analysis of spatial distribution of symptomatic plants, and then to develop a predictive model for the onset of the foliar symptoms of GLSD.

Materials and methods

Experimental site and climate data

The research was conducted on a 1.22 ha vineyard located in the Chianti Classico Domain (43°40′11.48″N-11°8′30.23″E) in Tuscany, Italy. The vineyard was planted in 1998 with Cabernet Sauvignon vines, with rows aligned NW-SE, 2.8 m between rows and the vines spaced 1.0 m apart within the rows. The vineyard was trained as upward vertical shoot positioning and pruned as spur cordons. Irrigation was not applied. The vineyard is located on a south exposed slope (8%) at 150 m above sea level. The experimental plot consisted of ten adjacent rows 50 m long, providing a sample of 500 vines to be monitored. This plot was chosen because of the high GLSD incidence (almost every year over 30% of vines affected) when monitored at the single plant level since 2003, without variability between vines in terms of vigour and of the land slope (less than 5%). Ground observations were collected between May and September, at weekly intervals in 2012, and at monthly intervals in 2013, while the UAV flight survey was made at full bloom (25 May 2012) as a preliminary flight, fruit-set (25 June 2012 and 2013) and beginning of veraison (25 July 2012 and 2013). Climate was characterized with agrometeorological data acquired from a MeteoSense weather station (Netsens srl) located 10 m from the East side of the vineyard.

Ground observation

All vines in the experimental plot were classified in the following categories: S = symptomatic vines with pronounced symptoms related to 20–100% disease severity; C = control vines that never showed foliar symptoms; or A = asymptomatic vines that had shown symptoms in the previous years. The vines that showed less than 20% disease severity were not included in the S category because the symptoms were generally located in basal leaves, which has low impact on yield quality and quantity and are barely detectable by the UAV flight survey. The ground disease monitoring was performed by two well-trained surveyors by observing the foliage of each vine, on both sides of each row, including branches, shoots and bunches. A percentage value for disease severity was ascribed using an arbitrary disease scale, where 0 = no symptoms; 1 = 0.1–10%; 2 = 11–20%; 3 = 21–40%; 4 = 41–60%; and 5 = 61–100%. The typical wood alterations associated with the esca complex were verified in a random sample of symptomatic vines (S category), by inspecting transverse stem sections as described in previously (Surico *et al.*, 2008).

Ground-based ecophysiological measurements

During the 2013 growing season, plant ecophysiological measurements on leaves and pruned wood were introduced. Stomatal conductance (gs) and leaf temperature were recorded using an infrared gas analyser LI-COR 6400 (LI-COR, Lincoln, NE, USA). To avoid the environment variability, Photosynthetic Active Radiation (PAR) was set at 1000 $\mu mol\ m^{-2}\ s^{-1}$, CO_2 air concentration at 400 ppm, and cuvette temperature at 30°C. Measurements were made in four fully expanded and even-aged leaves from five different plants per treatment from 09:00 to 16:00 h (solar time). Measurements considered only control (always asymptomatic) and asymptomatic (that showed symptoms in previous years) plants, because the leaves of symptomatic plants show large necrotic areas that do not allow correct measurement with the gas analyser.

Epidermal polyphenols, which are representative of total leaf phenols (Kolb and Pfundel, 2005; Barthod *et al.*, 2007), were non-destructively measured on the same sample leaves using a portable leaf-clip device (Dualex; Force-A, Orsay, France). This determines epidermal absorbance in the UV-A wavelength (315–400 nm), which is mainly due to flavonoids (Goulas

et al., 2004; Cartelat *et al.*, 2005). Two adaxial and two abaxial measurements were recorded in sequence from the middle part of each leaf avoiding the main veins, and flavonoid contents was calculated following the method of Pollastrini *et al.*, (2011).

As a further test to evaluate differences among the three vine classes (Symptomatic, Asymptomatic, Control), the distance between nodes and the weight of the canes were measured as indicators of the rate of shoot growth during the 2012 season (Pratt, 1974; Mullins *et al.*, 1992). In January 2013 a cane was collected from of each vine from 30 vines from each of the three vine classes (S, A, C). The cane portion between the 2nd and 7th node from the base of each 1-year-old cane grown was selected in the 2012 growing season to measure length and fresh weight.

Unmanned aerial platform

Multispectral images were acquired with a UAV platform, based on a modified multi-rotor Mikrokopter OktoXL (HiSystems GmbH) equipped with a nadir-facing Tetracam ADC-lite camera (Tetracam, Inc.) (Figure 2a). The camera weighed 200 g and had remote power and display features for optimized placement on UAV platforms. The primary use of this camera is to record vegetation canopy reflectance for derivation of several vegetation indices (NDVI, Soil Adjusted Vegetation Index, canopy segmentation and Near Infrared/Green ratios). Images were recorded in the visible red (R) wavelength (520–600 nm) and green (G; 630–690) and near infrared (NIR; 760–900 nm) spectra. Camera features such as 3.2 megapixel CMOS sensor (2048 ´ 1536 pixels), 8.5 mm lens and 43° field of view, provided a 0.05 m/pixel ground resolution at a flight height of 150 m. All images were taken between 12:00 and 13:00 h (solar time) each day, in clear sky conditions. A white reference image was taken to compute reflectance by framing a Teflon calibration panel just before take-off. The flight altitude was fixed at 150 m (above ground level), and the UAV flight speed was of 4 m s^{-1}. These settings allowed a 72% image forward overlap, while a waypoints route planned *ad hoc* ensured a 40% image side overlap, great enough to guarantee optimal photogrammetric processing. The UAV platform, camera features and image processing were described previously (Matese *et al.*, 2015). Sample plants were georeferenced at high resolution (0.02 m) with a differential GPS (Leica GS09 GNSS, Leica Geosystems AG) to precisely discriminate vines along the rows (Figure 2b).

Figure 2. Instrumentation used in the study. A, Multirotor UAV platform (Mikrokopter, HiSystems GmbH, Moomerland, Germany), inset shows the multispectral camera (Tetracam ADC-Lite, Tetracam), B, Differential GPS (Leica GS09 GNSS, Leica Geosystems AG).

Data processing

PixelWrench2 software (Tetracam Inc.) was used to manage and process multispectral images, providing a batch file conversion from RAW to TIFF. Two captured images were assembled into a mosaic by Autopano Pro 3.6 Software (Kolor SARL,). Twenty white PVC panels, each of 0.25 × 0.25 m, were used as Ground Control Points (GCPs) and located at the beginning and end of each vine row of the plot. The panels were georeferenced in the field during image acquisition using the high-resolution differential GPS.

The QGIS software (Quantum GIS Development Team 2014, Quantum GIS Geographic Information System, Open Source Geospatial Foundation Project, http://qgis.osgeo.org) was used to georeference the mosaics utilizing GCP white panel coordinates in the georeferencing plugin. A thin plate spline (TPS) function was applied using a nearest neighbor resampling method to render the geometrically corrected mosaic. NDVI values were then calculated from the multispectral mosaic. Data extraction for single plants was performed from the NDVI maps with an *ad hoc* developed algorithm on Matlab software platform (MATLAB version 7.11.0.584, (2010), The MathWorks Inc.), by means of average values contained in 0.80 × 0.30 m polygons along the row axes, centered on each georeferenced vine. The polygon size was chosen in order to better distinguish each plant from the adjacent ones, providing a buffer of 0.40 m between consecutive vines as a consequence of the vine spacing of 1.0 × 2.8 m. The homogeneity of the canopy and the availability of high spatial resolution images allowed correct extraction of the pure canopy pixels of sample vines, and verification of the exclusion of pixels of the underlying grass or bare soil.

Statistical analysis

Statistical analysis of the pruning wood (weight and length) and NDVI data, were analyzed by one-way ANOVA, with R Stat (R Project for Statistical Computing; www.R-project.org). Means were then separated using the Tukey's HSD test at $P{\leq}0.05$. Predictive power of UAV was statistically evaluated by comparing, for each flight of 2012, the symptom classes. Leaf parameters (stomatal conductance, leaf temperature and flavonoid content) were analyzed by one way ANOVA at $P{\leq}0.05$.

Results

Climate analysis

According to the Winkler index (Winkler et al., 1974; Hall and Jones 2010) and other bioclimatic indices (Huglin Index, Sum of daily temperature excursion, Gladstones Index, cumulative rainfall, sum of daily min, max and mean temperatures, number of days of temperatures over 35°C), the growing season of 2012 showed a higher thermal regime than 2013 (Table 1, Figure 3).

The 2012 growing season was dry, characterized by high temperatures (37 d above 35°C), minimum rainfall events concentrated in April and May and an extreme summer drought (no more than 50 mm of rain between June and August). The 2013 season, on the other hand, had high total rainfall well distributed throughout the year, with 200 Growing Degree Days, which was less than the previous year. 2013 was a wet season with moderate temperatures (only 12 d with temperatures above 35°C). In summary, analyzing the experimental period, conditions were similar during April and May in

Table 1. Bioclimatic indices during the period between the years 2012–2013.

Year	WI[a]	HI[a]	SET[a]	GI[a]	Rain[b] 01/03–31/08	min	ST[c] max	mean	Days Tmax>35°C[d] 01/03–31/08
2012	1915	2630	2364	1914	257	2668	5032	3739	37
2013	1715	2406	2246	1715	631	2553	4799	3541	12

[a] WI, Winkler Index; HI, Huglin Index; SET, Sum of daily temperature excursion; GI, Gladstones Index.
[b] Cumulative rainfall (01/03–31/08).
[c] ST, Sum of daily min, max and mean temperatures (STmin, STmax, STmean).
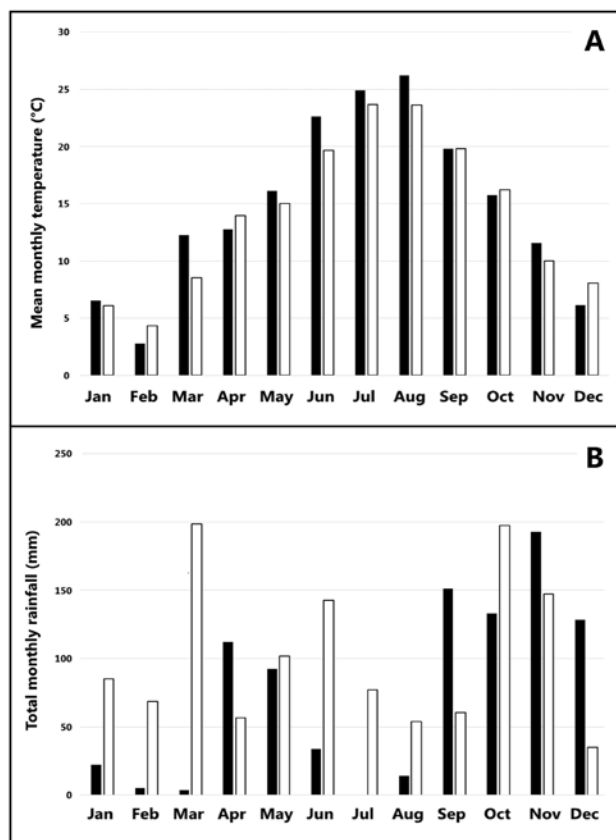[d] Number of days of temperatures over 35°C (01/03–31/08).

Figure 3. Climate analysis report. Climate data for 2012 (black) and 2013 (white): A, monthly mean temperature and B, total monthly rainfall.

both seasons, with moderate rainfall and moderate temperatures, while the summer months were hot and dry in 2012, while they were moderate and wet in 2013.

Image processing analyses

With the combined use of the UAV remote sensing platform and differential GPS, NDVI maps with high-resolution on the ground (0.05 m/pixels) were obtained. These allowed accurate analyses at single plant level. The algorithm developed in the Matlab platform allowed precise row identification and data extraction for each plant from the NDVI map (Figure 4). For each vine, base zonal statistics (mean, minimum, maximum and standard deviation) were calculated relative to each pixel contained inside the different polygons.

Comparison between field ground observation and UAV-based remote sensing NDVI

Stomatal conductance of leaves was significantly less in A vines compared to C vines, while leaf temperature in A vines was significantly greater than in C vines (Figure 5). Mean optical estimation of phenolic compounds showed significant differences between C and A vines (F = 28.16, $P \leq 0.0001$), with greater mean flavonoid values in the A vines (1.98 ± 0.10) compared with the C vine samples (1.85 ± 0.16).

The analysis of the pruning wood carried on the lengths and fresh weights of the shoots in the three vine classes showed that mean lengths of canes from C vines (49.7 cm ± 3.9) were significantly greater than those from A vines (46.1 cm ± 3.6; F = 13.8, $P<0.001$) and symptomatic (42.7 cm ± 3.6; F = 52.19, $P<0.001$) (Figure 6A). The mean weights of C vine canes (44.4 g ± 6.8) were significantly longer than those from A vines (32.1 g ± 6.6; F = 49.95, $P<0.001$) or S vines (25.9 g ± 5.0; F = 142.4, $P<0.001$) (Figure 6B). Mean weights and lengths of pruning wood showed a clear negative trend from C to S vines (Figure 6).

Figure 7 presents the NDVI values of the three vine classes (C, A and S) for 2012 and 2013, confirming this negative trend. Greater NDVI values were recorded for healthy vines (C) and lower NDVI values occurred for symptomatic vines (S). In both years, the asymptomatic plants (A) were characterized by lower NDVI values than healthy samples (C). NDVI values acquired in 2013 were greater than in the dryer 2012 season.

This trend could indicate a method to discriminate between possibly healthy vines and those that are known to be infected, since the asymptomatic vines had displayed GLSD foliar symptoms in the past. Anova analysis (Table 2) shows that the UAV approach correctly discriminated ($P \leq 0.05$) healthy vines from asymptomatic and symptomatic vines, and asymptomatic from symptomatic vines ($P \leq 0.05$) for each year, also in different meteorological conditions. The discrimination increased during each season: NDVI data analysis showed significant differences ($P \leq 0.05$) since the beginning of the monitoring period (May in 2012 and June in 2013), with maximum differences between each class in the last flight acquisition in July in both years ($P<0.001$).

This result suggests that further analysis should be carried out to determine if UAV remote sensing data can provide information about the onset of GLSD symptoms. Ground observations at weekly
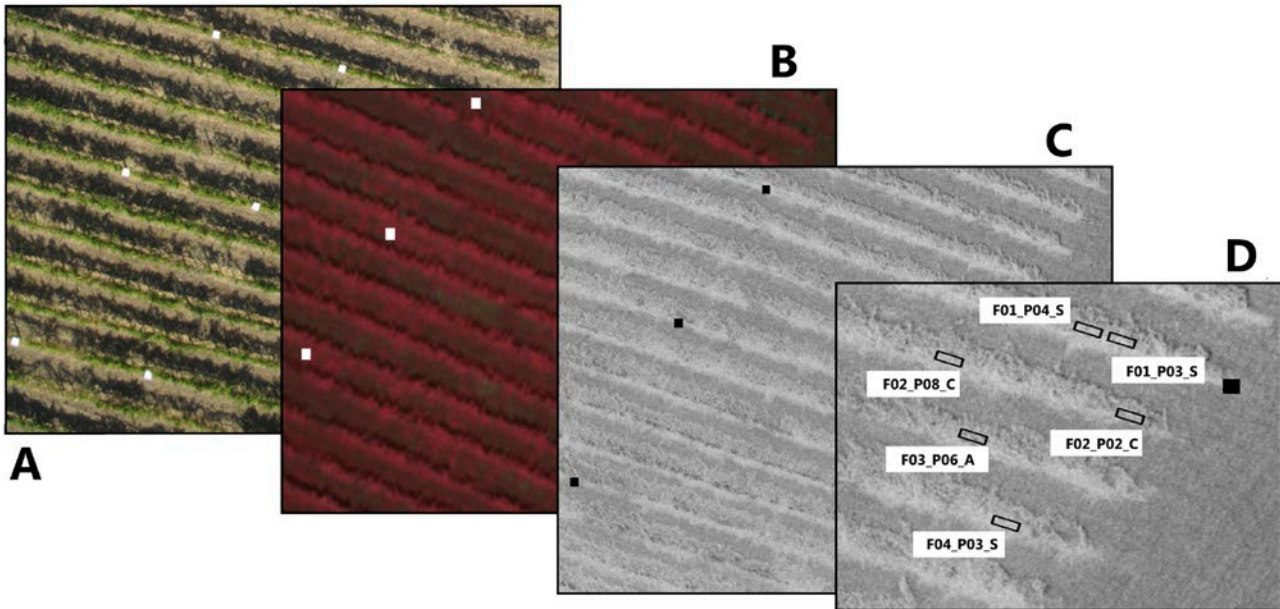
Figure 4. Image processing workflow. A, visible image, B, multispectral image, C, NDVI image, D, row detection and plant extraction data output.
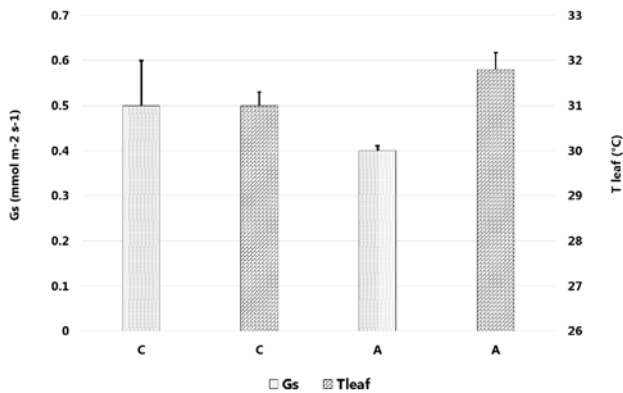

Figure 5. Ground-based ecophysiological measurements. Stomatal conductance (gs) and leaf temperature were recorded using an infrared gas analyser, on healthy (C) and asymptomatic (A) grapevines.

intervals were carried out in the 2012 season to produce accurate analysis of the predictive approach on the 2012 data. NDVI data of classes C (control), A (asymptomatic) and S (symptomatic) were compared to another class, that we define X, including only the vines that, despite being asymptomatic at the flight time, showed symptoms just 2–3 weeks af-

ter each UAV flight. Data analysis (Table 3) shows that the remote sensing methodology always identified apparently healthy vines that were going to show symptoms in the following few weeks. This approach had the best resolution ($P \leq 0.05$) both in June and July 2012, to discriminate C and X class, while no significant correlation could be detected in May. Furthermore the X class (vines going to be soon symptomatic) were quite close to the S class (symptomatic vines).

Discussion

Climate was identified as an important distinguishing element between the two growing seasons investigated in this study, and meteorological parameters are known to have a crucial influence on vegetative response of grapevines (Matese *et al.*, 2012). 2012 was a very low rainfall year, while 2013 had high rainfall which was well distributed throughout the season. This most likely stimulated the vegetative metabolism of the plants in 2013, which maintained a photosynthetic efficiency of the canopy until the end of September (Palliotti *et al.*, 2014). In 2012, on the other hand, the greatest NDVI values were reached in July. It is very likely that leaf
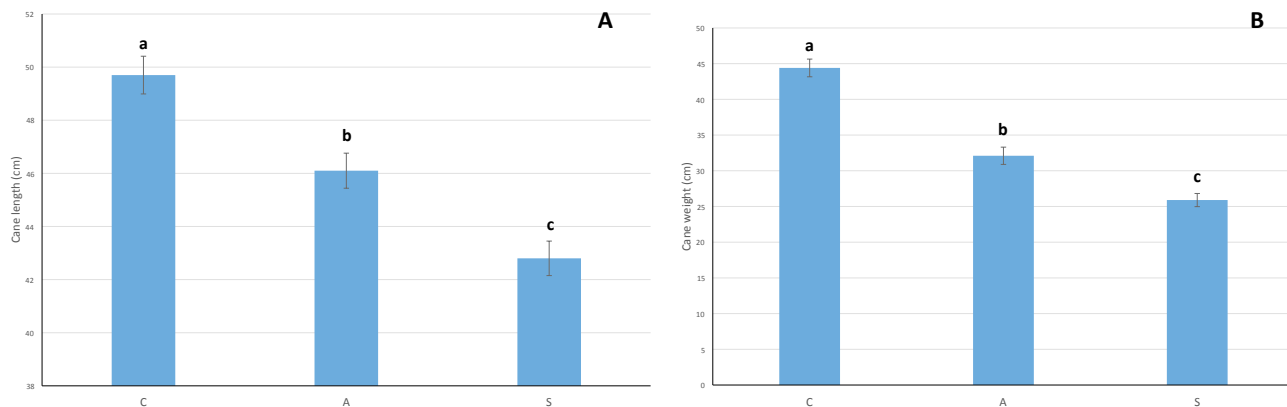
Figure 6. Mean lengths and fresh weights of the cane portion between the 2nd and 7th nodes from the base of canes grown in the 2012 season and collected at pruning in January 2013, from vines classified in the 2012 growing season in the three classes: control, always symptomatic or asymptomatic.
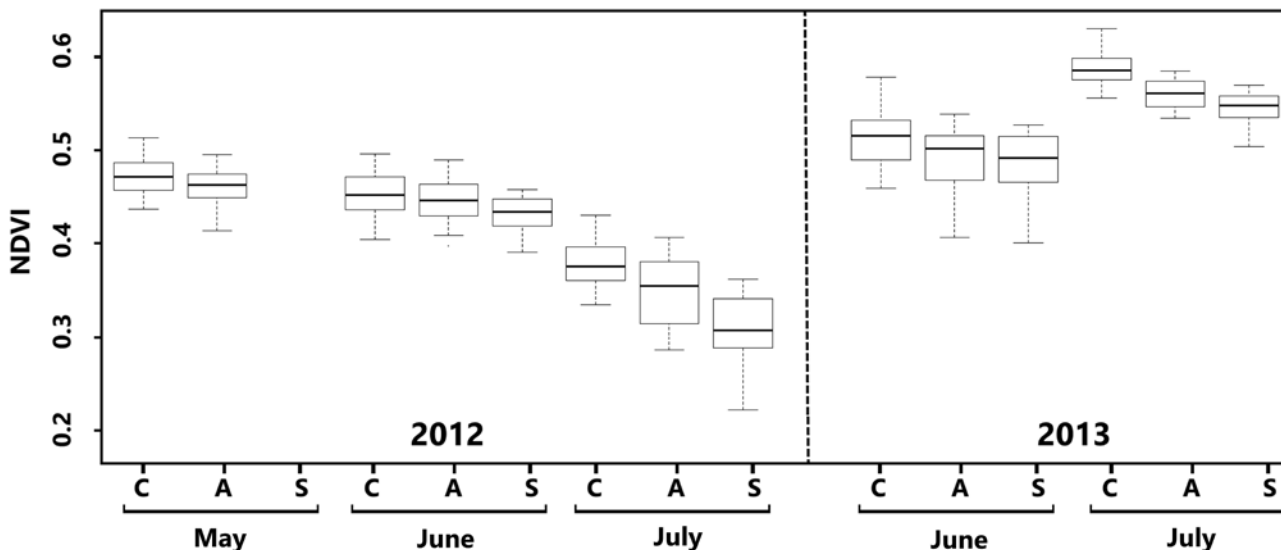

Figure 7. Relationship between NDVI data and ground observations. Boxplot graphical output of the correlation between NDVI values and GLSD symptoms for May, June and July of 2012 and 2013. The graph shows a negative trend in NDVI, with greater values in healthy vines (C) and lesser values in symptomatic vines (S), with intermediate values for the asymptomatic vines (A).

metabolism was affected by the disease history of the vines. Even when visually fully indistinguishable, leaves of asymptomatic vines had alterations (reduced stomatal conductance and increased leaf temperature; Petit *et al.* (2006)) that were related to the reduced NDVI values obtained by remote sensing. Differences between healthy and asymptomatic plants also emerged from the preliminary results on

epidermal polyphenol contents. The role of phenolic compounds in the defense mechanism protecting grapevine against the fungi involved in esca disease, and against grapevine pathogens in general, has been well explored by several authors (Del Rio *et al.*, 2004; Lattanzio *et al.*, 2006; Amalfitano *et al.*, 2011; Lambert *et al.*, 2012). It could be hypothesized that the accumulation of flavonoids within the asympto-

Table 2. Detection power of UAV methodology was statistically evaluated (one-way ANOVA, Tukey's HSD test at $P \leq 0.05$) by comparing for each flight of 2012 and 2013, NDVI data of classes C (control), A (asymptomatic) and S (symptomatic).

Plant category	May 2012	June 2012	July 2012	June 2013	July 2013
Control	a	a	a	a	a
Asymptomatic	b	b	b	b	b
Symptomatic	n.d. [a]	c	c	c	c

[a] n.d., no symptomatic vines detected in May 2012.

Table 3. Predictive power of UAV was statistically evaluated (one-way ANOVA, Tukey's HSD test at $P \leq 0.05$) by comparing, for each flight of 2012, classes C (control), A (asymptomatic), X (asymptomatic vines at flight time that showed symptoms 2–3 weeks after the flight) and S (symptomatic).

Plant category	May 2012	June 2012	July 2012
C	a	a	a
A	a	b	ab
X	a	bc	b
S	n.d. [a]	c	b

[a] See Table 2.

matic plant leaves is the response of infected plants that have been able to prevent the manifestation of symptoms during the growing season.

The statistical analyses of the data collected in 2012 and 2013 shows that the very high resolution multispectral images acquired by UAV can discriminate different stress levels in grapevines, in relation to the visual symptoms of GLSD. In particular, Figure 7 shows good distinction between healthy plants (C) and symptomatic plants (S) in both years of this study, despite the different climatic conditions of the two growing seasons. The characterization of asymptomatic plants (A) is still relatively unexplored in the literature, but preliminary results confirm that the median of values of NDVI of asymptomatic vines is in an intermediate position with respect to the median of the other two disease classes, although with a partial overlap of boxplots. This

intermediate position also clearly emerges from the data of cane lengths and weights obtained during a season when vines had been symptomatic, asymptomatic, disease-free ("control" vines). It is well known that a vine showing symptoms one growing season may not show symptoms in the next, and continues to give good quality wine. Nevertheless, the vigour of these vines is affected, as growth and wood production are reduced, with a clear trend in these parameters from control to symptomatic vines. Cane weights and lengths were less for the symptomatic vines, as expected, greater for the control vines that had never showed symptoms, and intermediate in the asymptomatic vines which had bee previously symptomatic vines. These data relate closely to the NDVI gradient recorded using UAV-assisted remote sensing.

The analysis of meteorological conditions confirmed substantial differences between the two seasons (Table 1), which were reflected in plant vigour. The 2012 season, was characterized by high temperatures and minimal precipitation, and produced significantly lower NDVI values than recorded in the 2013 season (Figure 5). Table 2 shows differences between healthy and diseased plants, but these differences were more evident when the foliar symptoms drastically lowered the photosynthetic efficiency, and were most pronounced in July, when symptoms progressively increased on the foliage. Table 3 explores an experimental approach where the sample of plants was reduced to consider only the plants that would manifest symptoms after 2–3 weeks. The sample is limited to about 15–20 plants per month, but this confirms the findings of other authors (Bertamini *et al.*, 2002; Christen *et al.*, 2007; Letousey *et al.*, 2010; Mattii *et al.*, 2010; Magnin-Robert *et a1.*, 2011; Calamai *et al.*, 2014). They showed that alteration of the photosynthetic activity of the leaves occurs a few weeks before the onset of GLSD symptoms, suggesting that further exploration of remote sensing methodology could be useful for the development of disease forecasting methods and further potential applications. In the present study, a homogeneous vineyard plot was used that was small, but had been monitored since 2003 at single plant level. This was to reduce other variables that could alter the data analyses. In this way it was possible to attribute changes of photosynthetic efficiency of the canopy to the onset of GLSD symptoms by excluding other potential causes of biotic or abiotic stresses. The

experimentation used here explored the relationship between remotely acquired NDVI values, and symptoms of GLSD obtained by visual observation of both the symptomatic plants and those that were asymptomatic in the year in which the field survey was carried out. These asymptomatic plants would have been incorrectly considered as healthy plants if the disease history of the vineyard was not known.

Conclusions

The methodology outlined in this paper has produced valuable results that indicate new possibilities for the use of remote sensing technologies for precision viticulture. UAV features, such as low cost, capability of timely provision of high resolution images, and flexibility of use in flight planning, provide an approach that can be easily applied for investigation and disease control strategy planning in vineyards. These methods are likely to be useful, both for research and for practical applications in wine production. The results of NDVI data analyses revealed in two growing seasons that asymptomatic vines in the year of the observation were distinguished from the plants that had never showed foliar symptoms from 2003 to 2013. This allowed the hypothesis that in the asymptomatic vines the spectral differences cannot be detected by in the human visible spectrum, but are detectable in the near-infrared wavelength (NIR) used by the detection system, and therefore can be identified and discriminated from the "healthy" vines (category "C"). However, additional experimentation will be required, across different growing seasons and climatic conditions, to validate and confirm this hypothesis, and to provide a useful tool for elucidating complex and not fully understood disease. Analysis of NDVI images could allow prompt identification of the early stages of the symptoms, even before they can be visually detected. However, the NDVI measurements have clear limits, because they provide indices capable of identifying alterations in photosynthetic efficiency, but do not discriminate the causes of biotic or abiotic stress afflicting plants. Our work has been possible because the experimentation could be carried out on a sample of plants monitored in detail, so that other causes of stress could be eliminated, confirming that alterations of NDVI were exclusively linked to symptoms of GLSD. It will also be possible to integrate our system with new optical technologies such as a hyperspectral camera. This powerful sensor allows qualitative measures on symptomatic leaf spectral responses with very high detail. A future perspective will be to identify the spectral signature specific for GLSD symptoms, to strictly discriminate GLSD from other vineyard stresses or diseases. Early detection could also support the planning and testing of economically rewarding field treatments, or the application of specific control methods on the single vines before they show the symptoms. The applications of such a predictive tool could open new perspectives in the knowledge and control of this important grapevine disease, within the increasing development of the precision agriculture approaches in viticulture.

Acknowledgments

Literature cited

Amalfitano C., D. Agrelli, A. Arrigo, L. Mugnai, G. Surico and A. Evidente, 2011. Stilbene polyphenols in the brown red wood of *Vitis vinifera* cv. Sangiovese affected by" esca proper". *Phytopathologia Mediterranea* 50, 224–235.

Andolfi A., A. Cimmino, L. Mugnai, J. Luque, G. Surico, and A. Evidente, 2011. Phytotoxins produced by fungi associated with grapevine trunk diseases. *Toxins* 3, 1569–1605.

Andreini, L., R. Cardelli, S. Bartolini, G. Scalabrelli and R. Viti, 2015. Esca symptoms appearance in *Vitis vinifera* L.: influence of climate, pedo-climatic conditions and rootstock/cultivar combination. *VITIS-Journal of Grapevine Research* 53 (1), 33.

Baluja J., M. P. Diago, P. Balda, R. Zorer, F. Meggio, F. Morales and J. Tardaguila, 2012. Assessment of vineyard water status variability by thermal and multispectral imagery using an Unmanned Aerial Vehicle (UAV). *Irrigation Science* 30, 511–522.

Barthod S., Z.G. Cerovic and D. Epron, 2007. Can dual chlorophyll fluorescnce excitation be used to asses the variation

in the content of UV absorbing phenolic compounds in leaves of temperate tree species along an irradiance gradient? *Journal of Experimental Botany* 58, 1753–1760.

Bauer S.D., F. Korč and Förstner W., 2011. The potential of automatic methods of classification to identify leaf diseases from multispectral images. *Precision Agriculture* 12, 361–377.

Bellow S., G. Latouche, S.C. Brown, A. Poutaraud and Z.G. Cerovic, 2013. Optical detection of downy mildew in grapevine leaves: daily kinetics of autofluorescence upon infection. *Journal of Experimental Botany* 64, 333–341.

Blakeman R.H., 1990. The identification of crop disease and stress by aerial photography. Pages 229–254 in: *Application of Remote Sensing in Agriculture*. (Steven M.D., Clark J.A., ed.), Butterworths, London, UK.

Blazquez C.H. and G.J. Edwards, 1983. Infrared color photography and spectral reflectance of tomato and potato diseases. *Journal of Applied Photography Engeneering* 9, 33–37.

Berdugo C.A., R. Zito, S. Paulus and A.K. Mahlein, 2014. Fusion of sensor data for the detection and differentiation of plant diseases in cucumber. *Plant Pathology* 63, 1344–1356.

Bertamini M., K. Muthuchelian and N. Nedunchezhian, 2002. Iron deficiency induced changes on the donor side of PS II in field grown grapevine (*Vitis vinifera* L. cv. Pinot noir) leaves. *Plant Science* 162, 599–605.

Bertsch C., M. Ramírez-Suero, M. Magnin-Robert, P. Larignon, J. Chong, E. Abou-Mansour and F. Fontaine, 2013. Grapevine trunk diseases: complex and still poorly understood. *Plant Pathology* 62, 243–265.

Bravo C., D. Moshou, J. West, A. McCartney and H. Ramon, 2003. Early disease detection in wheat fields using spectral reflectance. *Biosystems Engineering* 84, 137–145.

Burns B.E., M.J. Starzyk and D.L. Lynch, 1969. Detection of plant virus symptoms with infrared photography. *Transactions of the Illinois State Academy of Science* 62, 102–105.

Calamai L., A. Goretti, G. Surico and L. Mugnai, 2014. Grapevine leaf stripe disease: a metabolomic approach by GC-MS identifies affected vines before symptom appearance. 9th International Workshop on Grapevine Trunk Diseases, National Wine Centre of Australia, Adelaide 18–20 November 2014. *Phytopathologia Mediterranea* 53, 580 (abstract).

Calderón R., J.A. Navas-Cortés, C. Lucena and P.J Zarco-Tejada, 2013. High-resolution airborne hyperspectral and thermal imagery for early detection of Verticillium wilt of olive using fluorescence, temperature and narrow-band spectral indices. *Remote Sensing of Environment* 139, 231–245.

Calzarano F., S. Di Marco and Cesari A., 2004a. Benefit of fungicide treatment after trunk renewal of vines with different types of esca necrosis. *Phytopathologia Mediterranea* 43, 116–123.

Calzarano F., L. Seghetti, M. Del Carlo and A. Cichelli, 2004b. Effect of esca on the quality of berries, musts and wines. *Phytopathologia Mediterranea* 43, 125–135.

Calzarano F. and S. Di Marco, 2007. Wood discoloration and decay in grapevines with esca proper and their relationship with foliar symptoms. *Phytopathologia Mediterranea* 46, 96–101.

Calzarano F., S. Di Marco, V. D'Agostino, S. Schiff, and L. Mugnai, 2014. Grapevine leaf stripe disease symptoms (esca complex) are reduced by a nutrients and seaweed mixture. *Phytopathologia Mediterranea* 53, 543–558.

Cartelat A., Z.G. Cerovic, Y. Goulasa, S. Meyera and C. Lelarge, 2005. Optically assessed contents of leaf polyphenolics and chlorophyll as indicators of nitrogen deficiency in wheat (*Triticum aestivum* L.). *Field Crops Research* 91, 35–49.

Christen D., S. Shonmann, M. Termini, R. J. Strasser, and G. Défago, 2007. Characterization and early detection of grapevine (*Vitis vinifera*) stress responses to esca disease by in situ chlorophyll fluorescence and comparison with drought stress. *Environmental and Experimental Botany* 60, 504–514.

Colomina I. and P. Molina, 2014. Unmanned aerial systems for photogrammetry and remote sensing: A review. *ISPRS Journal of Photogrammetry and Remote Sensing* 92, 79–97.

Darrieutort G. and P. Lecomte, 2007. Evaluation of a trunk injection technique to control grapevine wood diseases. *Phytopathologia Mediterranea* 46, 50–57.

Del Río J.A., P.Gómez, V. Frías, M.D. Fuster, A. Ortuño and A. Báidez, 2004. Phenolic compounds have a role in the defense mechanism protecting grapevine against the fungi involved in petri disease**.** *Phytopathologia Mediterranea* 43, 87–94.

Delalieux S., J.A.N. Van Aardt, W. Keulemans, E. Schrevens and P. Coppin, 2007. Detection of biotic stress (*Venturia inaequalis*) in apple trees using hyperspectral data: nonparametric statistical approaches and physiological implications. *European Journal of Agronomy* 27, 130–143.

Delalieux S., A. Auwerkerken, W. W. Verstraeten, B. Somers, R. Valcke, S. Lhermitte, J. Keulemans and P. Coppin, 2009. Hyperspectral reflectance and fluorescence imaging to detect scab induced stress in apple leaves. *Remote Sensing* 1, 858–874.

Di Marco S., F. Osti, F. Calzarano, R. Roberti, A. Veronesi and C. Amalfitano, 2011a. Effects of grapevine applications of fosetyl-aluminium formulations for downy mildew control on "esca" and associated fungi. *Phytopathologia Mediterranea* 50, 285–299.

Di Marco S., F. Osti and L. Mugnai, 2011b. First studies on the potential of a copper formulation for the control of leaf stripe disease within esca complex in grapevine. *Phytopathologia Mediterranea* 50, S300–S309.

Elarab M., A.M. Ticlavilca, A.F. Torres-Rua, I. Maslova and M. McKee, 2015. Estimating chlorophyll with thermal and broadband multispectral high resolution imagery from an unmanned aerial system using relevance vector machines for precision agriculture. *International Journal of Applied Earth Observation and Geoinformation* 43, 32–42.

Fitzgerald G.J., S.J. Maas and W.R. Detar, 2004. Spider mite detection and canopy component mapping in cotton using hyperspectral imagery and spectral mixture analysis. *Precision Agriculture* 5, 275–289.

Fontaine F., C. Pinto, J. Vallet, C. Clément, A.C. Gomes and A. Spagnolo, 2016. The effects of grapevine trunk diseases (GTDs) on vine physiology. *European Journal of Plant Pathololgy* 144, 707–721.

Goulas Y., Z.G. Cerovic, A. Cartelat and I. Moya, 2004. Dualex:

a new instrument for field measurements of epidermal UV-absorbance by chlorophyll fluorescence. *Applied Optics* 43, 4488–4496.

Graeff S., J. Link and W. Claupein, 2006. Identification of powdery mildew (*Erysiphe graminis* sp. *tritici*) and take-all disease (*Gaeumannomyces graminis* sp. *tritici*) in wheat (*Triticum aestivum* L.) by means of leaf reflectance measurements. *Central European Journal of Biology* 1, 275–288.

Gramaje D., L. Moster, J.Z. Groenewald and P.W. Crous, 2015. *Phaeoacremonium*: from esca disease to phaeohyphomycosis. *Fungal Biology* 119, 759–783.

Gubler W.D., L. Mugnai and G. Surico, 2015. Esca, Petri and grapevine leaf stripe diseases. Pages 52–57, in: *Compendium of Grape Diseases, Disorders, and Pests*, 2nd Edition. (Wilcox W.F., Gubler W.D., Uyemoto J.K., ed.), American Phytopathological Society Press, S. Paul, MN, USA.

Guérin-Dubrana L., A. Labenne, J.C. Labrousse, S. Bastien, R.E.Y. Patrice and A. Gégout-Petit, 2012. Statistical analysis of grapevine mortality associated with esca or eutypa dieback foliar expression. *Phytopathologia Mediterranea* 52, 276–288.

Hall A. and G. Jones, 2010. Spatial analysis of climate in wine-grape–growing regions in Australia. *Australian Journal of Grape Wine Research* 16, 389–404.

Hall A., J.P. Louis and D.W. Lamb, 2003. Characterising and mapping vineyard canopy using high-spatial-resolution aerial multispectral images. *Computers & Geosciences* 29, 813–822.

Hatfield P.L. and Jr P.J. Pinter, 1993. Remote sensing for crop protection. *Crop Protection* 12, 403–413.

Huang W., D.W. Lamb, Z. Niu, Y. Zhang, L. Liu and J. Wang, 2007. Identification of yellow rust in wheat using in-situ spectral reflectance measurements and airborne hyperspectral imaging. *Precision Agriculture* 8, 187–197.

Johnson L.F., B.M. Lobitz, R. Armstrong, R. Baldy, E. Weber, J. DeBenedictis and D. Bosch, 1996. Airborne imaging aids vineyard canopy evaluation. *California Agriculture* 50, 14–18.

Johnson L.F., S. Herwitz, S. Dunagan, B. Lobitz, D. Sullivan and R. Slye, 2003a. Collection of ultra high spatial resolution image data over California vineyards with a small UAV. *Proceedings 30th International Symposium on Remote Sensing of Environment,* 10–14 November, Honolulu, HI.

Johnson L.F., D. Roczen, S. Youkhana, R. Nemani and D. Bosch, 2003b. Mapping vineyard leaf area with multispectral satellite imagery. *Computers and Electronics in Agriculture* 38, 33–44.

Kolb C.A. and E.E. Pfundel, 2005. Origins of non-linear and dissimilar relationships between epidermal UV absorbance and UV absorbance of extracted phenolics in leaves of grapevine and barley. *Plant Cell and Environment* 25, 580–590.

Kurschner E., H. Walter and W. Koch, 1984. Measurements of spectral reflectance of leaves as a method for assessing the infestation with powdery mildew. *Journal Plant Disease Protection* 91, 71–80.

Lafon R., 1921. L'apoplexie, traitement préventif (Méthode Poussard), traitement curatif. In: *Modifications à Apporter à la Taille de la Vigne dans les Charentes - Taille Guyot-Poussard Mixte et Double*. Montpellier Roumégoux et Déhan, Montpellier, France, 96 pp.

Lambert C., J. Bisson, P. Waffo-Téguo, Y. Papastamoulis, T. Richard, M. F. Corio-Costet and S. Cluzet, 2012. Phenolics and their antifungal role in grapevine wood decay: focus on the Botryosphaeriaceae family. *Journal of Agricultural and Food Chemistry* 60, 11859–11868.

Larsolle A. and H.H. Muhammed, 2007. Measuring crop status using multivariate analysis of hyperspectral field reflectance with application to disease severity and plant density. *Precision Agriculture* 8, 37–47.

Lattanzio V., V.M.T. Lattanzio and A. Cardinali, 2006. Role of phenolics in the resistance mechanisms of plants against fungal pathogens and insects. *Phytochemistry: Advances in Research* 661, 23–67

Lecomte P., G. Darrieutort, J.M. Liminana, G. Comont, A. Muruamendiaraz, F.J. Legorburu and M. Fermaud, 2012. New insights into esca of grapevine: the development of foliar symptoms and their association with xylem discoloration. *Plant Disease* 96, 924–934.

Letousey P., F. Baillieul, G. Perrot, F. Rabenoelina, M. Boulay, N. Vaillant-Gaveau, C. Clément and F. Fontaine, 2010. Early events prior to visual symptoms in the apoplectic form of grapevine esca disease. *Phytopathology* 100, 424–431.

Lorrain B., I. Ky, G. Pasquier, M. Jourdes, L. G. Dubrana, L. Gény and P.L. Teissedre, 2012. Effect of Esca disease on the phenolic and sensory attributes of Cabernet Sauvignon grapes, musts and wines. *Australian Journal of Grape Wine Research* 18, 64–72.

Magnin-Robert M., P. Letousey, A. Spagnolo, F. Rabenoelina, L. Jacquens, L. Mercier, C. Clément and F. Fontaine, 2011. Leaf stripe form of esca induces alteration of photosynthesis and defence reactions in presymptomatic leaves. *Functional Plant Biology* 38, 856–66.

Manzer F.E. and G.R. Cooper, 1967. Aerial photographic methods of potato disease detection. *Maine Agricultural Experimental Station Bulletin* 646, 1–14.

Marchi G., F. Peduto, L. Mugnai, S. Di Marco, F. Calzarano and G. Surico, 2006. Some observations on the relationship on manifest and hidden esca to rainfall. *Phytopathologia Mediterranea* 45, 117–126.

Martinelli F., R. Scalenghe, S. Davino, S. Panno, G. Scuderi, P. Ruisi, P. Villa, D. Stroppiana, M. Boschetti, L.R. Goulart, *et al.*, 2015. Advanced methods of plant disease detection. A review. *Agronomy for Sustainable Development* 35, 1–25.

Matese A., A. Crisci, S.F. Di Gennaro, E. Fiorillo, J. Primicerio, P. Toscano, F.P. Vaccari, S. Di Blasi and L. Genesio, 2012. Influence of canopy management practices on vineyard microclimate: definition of new microclimatic indices. *American Journal Enology Viticulture* 63, 424–430.

Matese A., P. Toscano, S.F. Di Gennaro, L. Genesio, F.P. Vaccari, J. Primicerio, C. Belli, A. Zaldei, R. Bianconi and B. Gioli, 2015. Intercomparison of UAV, aircraft and satellite remote sensing platforms for precision viticulture. *Remote Sensing* 7, 2971–2990.

Mathews A.J., 2014. Object-based spatiotemporal analysis of vine canopy vigor using an inexpensive unmanned aerial vehicle remote sensing system. *Journal of Applied Remote Sensing* 8, 085199, 1–17.

Mathews A.J., 2015. A practical UAV remote sensing methodology to generate multispectral orthophotos for vineyards: Estimation of spectral reflectance using compact digital cameras. *International Journal of Applied Geospatial Research* 6, 65–87.

Mattii G.B., E. Bardi, C. Calabrese and A. Giorgini, 2010. Alterazioni degli scambi gassosi causati dal mal dell'esca - misurazioni su foglia singola e sull'intera chioma di piante di vite in vaso. Pages 241–260, in: *Il mal dell'Esca della Vite: Interventi di Ricerca e Sperimentazione per il Contenimento Della Malattia*. (Surico G., L. Mugnai, ed.)., Progetto Mes-Vit. Arsia Regione Toscana, Firenze, Italy.

Mirik M., R.J. Ansley, J.A. Price, F. Workneh and C.M. Rush, 2013. Remote monitoring of wheat streak mosaic progression using sub-pixel classification of Landsat 5 TM imagery for site specific disease management in winter wheat. *Advanced in Remote Sensing* 2, 16–28.

Mugnai L., A. Graniti and G. Surico, 1999. Esca (Black Measles) and brown wood-streaking: two old and elusive diseases of grapevines. *Plant Disease* 83, 404–418.

Mullins M.G., A. Bouquet and L.E. Williams, 1992. *Biology of the Grapevine*. Cambridge University Press, Cambridge, UK, 239 pp.

Naidu R.A., E.M. Perry, F.J. Pierce and T. Mekuria, 2009. The potential of spectral reflectance technique for the detection of Grapevine leafroll-associated virus-3 in two red-berried wine grape cultivars. *Computers and Electronics in Agriculture* 66, 38–45.

Palliotti A., S. Tombesi, T. Frioni, F. Famiani, O. Silvestroni, M. Zamboni and S. Poni 2014. Morpho–structural and physiological response of container-grown Sangiovese and Montepulciano cv. (*Vitis vinifera*) to re-watering after a pre-veraison limiting water deficit. *Functional Plant Biology* 41, 634–647.

Peñuelas J. and I. Filella, 1998. Visible and near-infrared reflectance techniques for diagnosing plant physiological status. *Trends in Plant Science* 3, 151–156.

Pollastrini M., V. Di Stefano, M. Ferretti, G. Agati, D. Grifoni, G. Zipoli, S. Orlandini and F. Bussotti, 2011. Influence of different light intensity regimes on leaf features of *Vitis vinifera* L. in ultraviolet radiation filtered condition. *Environmental and Experimental Botany* 73, 108–115.

Pratt C., 1974. Vegetative anatomy in cultivated grapes. A review. *American Journal of Enology and Viticulture* 25, 131–150.

Reynolds G.J., C.E. Windels, I.V. MacRae and S. Laguette, 2012. Remote sensing for assessing Rhizoctonia crown and root rot severity in sugar beet. *Plant Disease* 96, 497–505.

Rouse J.W. Jr., R.H., Haas, J.A. Schell and D.W. Deering, 1973. Monitoring vegetation systems in the Great Plains with ERTS. Pages 309–317, in: *Proceedings of the 3rd ERTS Symposium*, NASA SP-351, 10–14 December, Washington, DC, USA.

Sankarana S., A. Mishraa, R. Ehsania and C. Davis, 2010. A review of advanced techniques for detecting plant diseases. *Computer Electronic Agriculture* 72, 1–13.

Smart R., 2015. Trunk diseases: Timely trunk renewal to overcome trunk disease. *Wine & Viticulture Journal* 30 (5), 44.

Steddom K., G. Heidel, D. Jones and C.M. Rush, 2003. Remote detection of Rhizomania in sugar beet. *Phytopathology* 93, 720–726.

Steddom K., M.W. Bredehoeft, M. Khan and C.M. Rush, 2005. Comparison of visual and multispectral radiometric disease evaluations of cercospora leaf spot of sugar beet. *Plant Disease* 89, 153–158.

Steven M.D. and J.A. Clark, 1990. *Applications of Remote Sensing in Agriculture*. (Steven M.D., Clark J.A., ed.), Butterworths, London, UK, pp 427.

Surico G., L. Mugnai and G. Marchi, 2008. The Esca Disease Complex. Pages 119–136, in: *Integrated Management of Diseases Caused by Fungi, Phytoplasma and Bacteria*. (Ciancio A., Mukerji K.G. ed.), Springer, Heidelberg, Germany.

Surico G., G. Marchi, P. Braccini and L. Mugnai, 2000. Epidemiology of esca in some vineyards in Tuscany (Italy). *Phytopathologia Mediterranea* 39, 190–205.

Thomas J. R. and G.F. Oerther, 1972. Estimating nitrogen content of sweet pepper leaves by reflectance measurements. *Agronomy Journal* 64, 11–13.

Toler R.W., B.D. Smith, J.C. Harlan, 1981. Use of aerial color infrared to evaluate crop disease. *Plant Disease* 65, 24–31.

Wang W., C. Thai, C. Li, R. Gitaitis, E. Tollner and S.C. Yoon, 2009. Detection of sour skin diseases in vidalia sweet onions using near-Infrared hyperspectral imaging. In: *Proceedings of 2009 ASABE Annual International Meeting*. 21–24 June, Reno, NV, USA.

West J.S., C. Bravo, R. Oberti, D. Lemaire, D. Moshou and H.A. McCartney, 2003. The potential of optical canopy measurement for targeted control of field crop diseases. *Annual Review of Phytopathology* 41, 593–614.

Winkler A., J. Cook, W. Kliewer and L. Lider, 1974. *General Viticulture*, 2nd ed. University of California Press, Berkeley, CA, USA, 710 pp.

Zaman-Allah M., O. Vergara, J.L. Araus, A. Tarekegne, C. Magorokosho, P.J. Zarco-Tejada, A. Hornero, A. Hernández Albà, B. Das, P. Craufurd, M. Olsen, B.M. Prasanna and J. Cairns, 2015. Unmanned aerial platform based multi spectral imaging for field phenotyping of maize. *Plant Methods* 11, 35.

Zhang N., M. Wang and N. Wang, 2002. Precision agriculture – a worldwide overview. *Computers and Electronics in Agriculture* 36, 113–132.